Article:
Shamsuddin, SH, Gibson, TD, Tomlinson, DC orcid.org/0000-0003-4134-7484 et al. (3 more authors) (2021) Reagentless Affimer- and antibody-based impedimetric biosensors for CEA-detection using a novel non-conducting polymer. Biosensors and Bioelectronics, 178. 113013. ISSN 0956-5663

https://doi.org/10.1016/j.bios.2021.113013

Title: Reagentless Affimer- and antibody-based impedimetric biosensors for CEA-detection using a novel non-conducting polymer

Shazana Hilda Shamsuddin[a,b,*], Timothy D. Gibson[a], Darren C. Tomlinson[c], Michael J. McPherson[c], David G. Jayne[d], Paul A. Millner[a]**

[a] The Leeds Bionanotechnology Group, School of Biomedical Sciences, University of Leeds, LS2 9JT, Leeds, United Kingdom
[b] Department of Pathology, School of Medical Sciences, Health Campus, Universiti Sains Malaysia, 16150, Kelantan, Malaysia
[c] Astbury Centre for Structural and Molecular Biology, University of Leeds, LS2 9JT, Leeds, United Kingdom
[d] Leeds Institute of Medical Research, University of Leeds, LS9 7TF, Leeds, United Kingdom

Correspondence and requests for materials should be addressed to *S.H.S. (email: shazana.hilda@usm.my) or **P.A.M. (email: P.A.Millner@leeds.ac.uk)

Abstract:

Polyoctopamine (POct), an amine-functionalised non-conducting polymer, as the transducer layer in an electrochemical biosensor, is presented. This polymer offers versatile covalent coupling either through thiol linker conjugation, carboxyl or aldehyde functional groups without the requirement of pre- or post-surface activation. The colorectal cancer biomarker carcinoembryonic antigen (CEA) was selected as the target analyte, whilst an antibody and a synthetic binding protein, an Affimer, were used as distinct bioreceptors to demonstrate the versatility of polyoctopamine as a transducer polymer layer for oriented immobilisation of the bioreceptors. The electrodeposited polymer layer was characterised using cyclic voltammetry, electrochemical impedance spectroscopy, and on-sensor chemiluminescent blotting. The performance of optimized POct-based biosensors were tested in spiked human serum. Results showed that the electropolymerisation of octopamine on screen printed gold electrode generates a thin polymer film with low resistance. Close proximity of the immobilised bioreceptors to the transducer layer greatly enhanced the sensitivity detection. The sensitivity of the smaller monomeric bioreceptor (Affimer, 12.6 kDa) to detect CEA was comparable to the dimeric antibody (150 kDa) with limit of detection at 11.76 fM which is significantly lower than the basal clinical levels of 25 pM. However, the Affimer-based sensor had a narrower dynamic range compared to the immunosensor (1 – 100 fM vs. 1 fM – 100 nM, respectively). All electrochemical measurements were done in less than 5 minutes with small sample volumes (10 µl). Hence, polyoctopamine features a simple fabrication of impedimetric biosensors using amine-functionalisation technique, provides rapid response time with enhanced sensitivity and label-free detection.

Keywords: Polyoctopamine; non-conducting polymer; oriented immobilisation; electrochemical immunosensor; Affimer; CEA

1. Introduction

Development of biosensors is pivotal in accelerating clinical diagnosis, notably for cancer detection and management since early cancer detection can be curative and can reduce morbidity and mortality (Arnold et al., 2017). Electrochemical biosensors, are the most developed presently and dominate the commercial market where they have been applied in clinical, and other fields (Hammond et al., 2016; Turner, 2013) due to their ease of use and minimal cost (Rushworth et al., 2013b) coupled with high specificity and sensitivity.

Two determinant factors in a biosensor device are transducer and bioreceptor. The binding of target analyte to the bioreceptor is converted into a measurable signal by the transducer (Thévenot et al., 2001). Currently, screen printed electrode (SPE) either from carbon or gold based are widely employed as the transducer due to low cost production. However, they inherent several limitations such as protein-based bioreceptor is prone to denaturation due to the hydrophobic nature of the electrode surface, and inconsistent biosensor performance due to uneven electrode surface generated from the screen printing (Ahmed et al., 2013; Jeuken, 2016). Therefore, in most circumstances, a polymer-based surface modification that can smoothen the interfacial surface and reduce roughness (Ahmed et al., 2013) and introduce additional functional groups such as amines, is necessary for immobilisation of the bioreceptor.

Conducting polymers (e.g. polypyrrole, polyaniline and polythiophene) provide electrical conductivity but suffer from thick conducting films and it can be difficult to control the redox states of the electropolymerised conducting polymers which leads to impedance instability (Ahmed, 2015; Goode, 2015). In comparison, phenol and its derivatives commonly produces a non-conducting polymer with low conductivity and high resistivity (Yuqing et al., 2004). The polymer growth is often self-limited during electropolymerisation and generates thinner films than with conducting polymers (10 -100 nm) (Tucceri, 2013). In the fabrication of electrochemical biosensors, the non-conducting polymer layer exhibits dual functions that are as immobilisation substrate with transducing elements (Ahmed et al., 2013; Yuqing et al., 2004). Polytyramine (Goode et al., 2016; Ismail and Adeloju, 2010) and the phenylenediamines (Stejskal, 2015) are typical examples of non-conducting polymers. These type of polymer are mainly used as transducer layers for molecular imprinted polymer (MIP)-based electrochemical biosensors (Gomes et al., 2018; Yarman et al., 2014) and enzyme-based biosensors (Cosnier and Holzinger, 2011; Pinyou et al., 2019). In the present study, the potential of polyoctopamine (POct), a phenol derivative with an extra hydroxyl group on its methylamine side

chain, was investigated as a novel non-conducting transducer polymer coating in the development of impedance biosensors for carcinoembryonic antigen (CEA) detection.

Apart from the transducer layer, selection of an appropriate bioreceptor is equally important for obtaining sensitive and effective biosensor operation and conventionally antibodies are employed due to their specific high affinity binding. However, they have inherent limitations such as stability, cost and batch variability and to circumvent these drawbacks, the alternative affinity binding protein, Affimer type II (Tiede et al., 2017; Tiede et al., 2014), has been developed. This binding protein is small (~13 kDa), monoclonal and based around a cystatin consensus sequence. Structurally it comprises one alpha helix and four anti-parallel β-strands. The two variable regions (VR), where molecular recognition occurs, resemble the CDR loops of antibodies and consist each of nine random amino acids (excluding cysteine). Affimer type II proteins were employed to fabricate the impedimetric biosensor in this study will herein be referred to as Affimer. In the past years, application of Affimer as biorecognition element in the development of biosensor was increasingly apparent. The applicability of Affimer in different category of biosensors were reported including electrochemical (Sharma et al., 2016; Thangsunan et al., 2021; Zhurauski et al., 2018), optical (Adamson et al., 2019) and mechanical (Koutsoumpeli et al., 2017).

CEA is the only blood–based protein biomarker that is widely utilised at present in clinical practice as a validated prognostic biomarker (Kim et al., 2009; Su et al., 2012) and as a diagnostic and surveillance biomarker for tumour recurrence in post-operative CRC patients (Labianca et al., 2010; Wu et al., 2010). It is also present in other adenocarcinomas (e.g. pancreatic, ovarian, breast, cervical and non-small-cell-lung cancers) with variable expression level (Beauchemin and Arabzadeh, 2013). The gold standard technique to detect CEA is by using enzyme linked immunosorbent assay (ELISA) with the cut-off value for CEA levels in serum considered abnormal is more than 5 ng/ml (equivalent to 25 pM) (Kim et al., 2009).

Published data of CEA biosensors showed that electrochemical biosensing is the most abundant approach compared to the other biosensor categories with amperometric biosensors being the most prominent technique, whilst voltammetric, impedimetric, capacitive and potentiometric measurements are less frequently used. These biosensors are based on a label-free detection technique using antibodies as the bioreceptors and randomly immobilised via amine-coupling (Liu and Ma, 2013; Sun et al., 2017; Xu et al., 2017). Labelled detection commonly showed better sensor performance but the overall fabrication of these biosensors was usually complex and time-consuming (Huang et al., 2018; Lv et al., 2018) which deviates from the objective of a POC application.

This study aimed to develop label-free electrochemical impedimetric biosensors on screen printed gold electrodes using POct as a novel non-conducting polymer layer for the detection of CEA. Here, we offer new evidence and validation of POct as a novel transducer layer with amine-functionalisation. Oriented immobilisation using various size of bioreceptors are easily fabricated with enhanced sensitivity. Study also showed efficacy and applicability of Affimer as an alternative bioreceptor for CEA detection.

2. Experimental

2.1. Reagents and apparatus

$NaIO_4$, NaH_2PO_4, $K_3Fe(CN)_6$ and $K_4Fe(CN)_6.3H_2O$, biotin-N-hydroxysuccinimide ester (biotin-NHS), octopamine hydrochloride, dimethyl sulfoxide (DMSO) and EDTA were from Sigma Aldrich (UK). Sulfosuccinimidyl 4-(N-maleimidomethyl) cyclohexane-1-carboxylate (Sulfo-SMCC), Glycolink coupling buffer pH 5.5, normal human sera, anti-CEA mouse monoclonal IgG antibody and Tris (2-carboxyethyl) phosphine (TCEP) disulphide reducing gels were from Thermo Scientific. Purified native CEA protein (Ab742) and goat-anti-mouse IgG HRP-conjugate was from Abcam plc. Sheep anti-digoxin IgG was from Therapeutic Antibodies UK Ltd whilst rabbit anti-CEA IgG was from Genscript Ltd. Human CEA ELISA assay kit was from Cusabio Technology LLC (Houston, USA). Anti-CEA and anti-Calprotectin Affimer containing a single cysteine at the C-terminal was isolated from the phage display library and has been characterised in affinity-fluorescent staining cells and pull-down assays (Shamsuddin et.al, article in press 2021). It will be used as an alternative biorecognition element in the fabrication of the biosensor.

Screen printed gold electrodes (SPGE) CX2223AT were purchased from DropSens (Asturias, Spain). As shown in **Fig. 1A,** the electrode has two round 1.6 mm gold working electrodes, a gold counter electrode and a Ag/AgCl reference electrode fired onto a ceramic base. Working electrode 1 (WE1, left) and 2 (WE2, right) were used to immobilise the non-specific and specific bioreceptors, respectively.

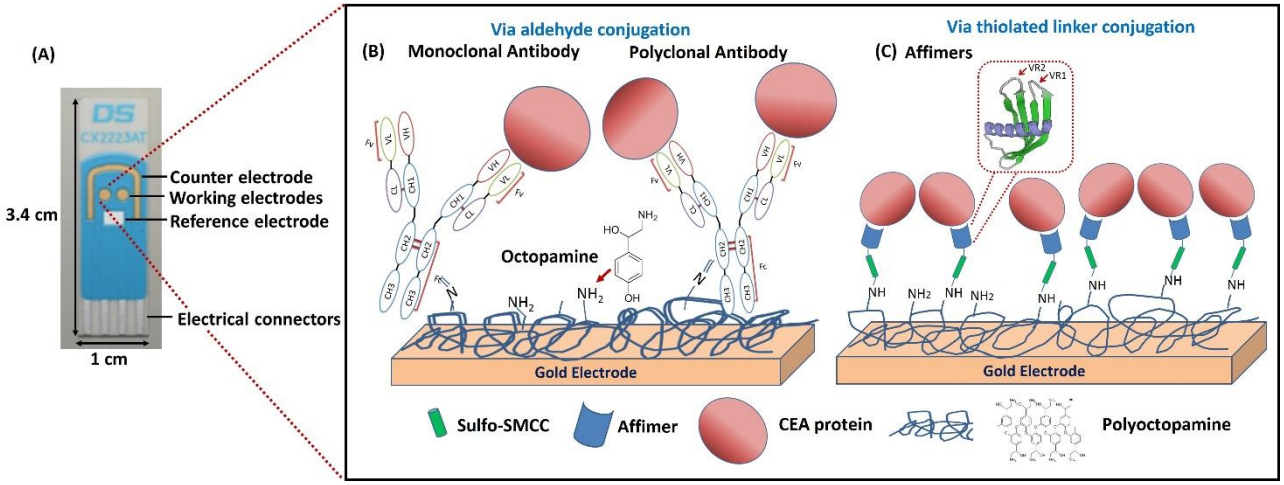

Fig. 1: Schematic of polyoctopamine based CEA biosensors construction

(A) DropSens screen printed gold electrodes with two round gold working electrodes, a gold counter electrode and a silver reference electrode; (B), oriented immobilisation of the oxidised antibodies onto POct film via covalent binding on DropSens screen printed gold electrode; (C), site-directed immobilisation of anti-CEA Affimer-II conjugated to polyoctopamine (POct) via sSMCC linker. Inset in (C) is the ribbon representation of Affimer (pdb ID: 4N6T). The drawing is not to scale.

2.2. Electrode preparation and functionalisation

2.2.1. Electropolymerisation of POct onto electrodes

A monomer solution of 5 mM octopamine in 100 mM phosphate buffer pH 7.5 and 20% (v/v) DMSO was electropolymerized onto DropSens working electrodes via cyclic voltammetry (CV) in the prepared solution with potential scanning between +0 V to +1.6 V and back at varies scan cycles (2, 4 and 6 cycles) and a range of scan rates (100 to 400 mV/s). Electrodes were washed thoroughly with 100 mM PBS pH 7.1 to remove excess octopamine monomer and incubated for 5 min in PBS prior functionalised with bioreceptors.

2.2.2. Biofunctionalisation of transducer surfaces for immunosensors

Antibody oligosaccharide was oxidised according to Wolfe and Hage (1995) using 10 mM $NaIO_4$ at pH 5.5 for 30 min to convert the carbohydrate on F_C into aldehyde groups. Freshly oxidized antibodies were diluted to 0.1 mg/ml in 100 mM phosphate buffer pH 7.1 and covalently bound to the amine groups on the working electrodes surface for 1 h at RT in a moist chamber. The modified electrodes were washed extensively with PBS and equilibrated for 30 min in PBS to obtain baseline signal stability. These fully constructed immunosensors were ready for electrochemical interrogation and testing for analyte binding. Monoclonal or polyclonal anti-CEA antibodies were used as specific receptors whilst anti-digoxin polyclonal antibody was used as a non-specific receptor. Both non-specific and specific receptors were immobilised separately onto working electrodes 1 and 2, respectively, in a single chip. **Fig. 1B** shows the schematic of immunosensors fabrication.

2.2.3. Electrochemical functionalisation of transducers for Affimer-based sensors

Fabrication of Affimer-based sensors comprised a step-wise process. This protocol has been previously patented by ELISHA Systems Limited (Gibson and Sharp, 2017). Initially, 20 mM octopamine solution was mixed with an equal volume of 26 mM sulfo-SMCC and allowed to react for 1 h at RT on a rotator. Both reagents were prepared in 100 mM phosphate buffer pH 7.5 and 20% (v/v) DMSO. Affimers containing a cysteine residue at the C-terminal region were reduced using immobilized TCEP reducing gel and diluted from stock in 100 mM phosphate buffer pH 7.1 prior to adding to the octopamide-SMCC conjugate. Freshly reduced Affimer at 0.2 mg/ml, was mixed with an equal volume of octopamide-SMCC conjugate and further incubated for 1 h at RT on a rotator. Electrochemical deposition of octopamide-SMCC-Affimer conjugate was then effected via CV using the same protocol as described above. Anti-CEA and anti-Calprotectin Affimers were used as the specific and non-specific bioreceptors that were immobilised separately onto working electrodes in the same manner a s the immunosensors. These fully functionalized sensor surfaces, either with or without blocking, were ready for electrochemical investigation and testing of CEA binding. Under optimum condition, the non-specific binding of fabricated Affimer sensor was blocked with 10 mM pyromellitic dianhydride (PMDA) in PBS pH 7.4 for 1 h at RT in a moist chamber prior to CEA interrogation. The schematic in **Fig. 1C** shows the fabrication of Affimer-based sensors.

2.2.4. On-sensor chemiluminescence analysis

Analysis of sensor surface throughout fabrication was performed by Midland blotting according to Rushworth et al. (2013a) to characterize the presence of functional groups created after polymerization and to validate the binding of the target analyte, CEA, on fully constructed sensors. For determination of surface amines after polymerisation of octopamine, modified electrodes were incubated in the presence or absence of biotin-NHS (2 µg/ml) for 1 h at RT in a moist chamber. The electrodes were washed once in 0.1% PBST and incubated for another 1 h in 1 µg/ml of streptavidin-HRP. These were followed by three washes in 0.1% PBST and four washes in 1×PBS prior to incubation in ECL reagent and immediate imaging using a Syngene G-Box imager. To evaluate the specific binding of CEA on fabricated Affimer sensors, monoclonal anti-CEA antibody and secondary antibody HRP conjugate were employed. The same washing steps and incubation with ECL reagent were performed. Images taken were further processed using ImageJ software. Original images captured were chemiluminescence (white light on a black background) but processed images are pseudo-green superimposed on chemiluminescence images for clarity.

2.2.5. Biosensor measurement of CEA

Biosensors either using antibodies or Affimers as bioreceptors were tested against a range of CEA concentrations by sequential additions of CEA in PBS pH 7.4 from 10^{-15} M to 10^{-7} M prior to incubation for 20 min in a moist chamber at RT. Electrodes were rinsed in 100 mM PBS pH 7.1 to remove any unbound analyte followed by electrochemical measurements. The optimised sensors were then tested in 1 % (v/v) to 0.001 % (v/v) normal human sera diluted in PBS pH 7.4.

Electrochemical measurements were conducted in a standard three cell system using a µAutolab type III electrochemical workstation fitted with a FRA2 frequency response (Metrohm Autolab B.V., Netherlands). Electrochemical impedance spectroscopy (EIS) analysis was used to investigate the fabricated sensors and to monitor CEA recognition. EIS measurements were carried out in 100 mM PBS pH 7.1 plus equal ratio of 10 mM $K_3[Fe(CN)_6]$/ $K_4[Fe(CN)_6]$. Impedance data were recorded from 2.5 KHz to 0.25 Hz with a modulation voltage of 10 mV at 0 V applied potential relative to the reference. Autolab NOVA software was used to analyse the collected data. Experiments were replicated ($n \geq 4$) on independent sensor surfaces. Change in charge transfer resistance (R_{CT}) was used to analyse the analyte binding activity on the sensor surface and to minimize the batch variability of the electrodes, the R_{CT} value of each concentration was normalized to the R_{CT} measured from the initial baseline of a fully constructed sensor in the absence of analyte using the following equation:

$$\text{Change in } R_{CT}\ (\%) = \frac{R_{CT}\ (\text{CEA}) - R_{CT}\ (\text{blank})}{R_{CT}\ (\text{blank})} \times 100$$

The limit of detection (LOD) was calculated based on the definition $LOD = mean_{blank} + 1.645(SD_{blank}) + 1.645(SD_{low\ concentration\ sample})$ (Armbruster and Pry, 2008)

3. Results and discussion

3.1. Surface characterisation of polyoctopamine modified screen printed gold electrodes

Electrochemical characterisation of polyoctopamine (POct) electrodeposited onto screen printed gold electrode was evaluated via cyclic voltammetry (CV) and electrochemical impedance spectroscopy (EIS). Initially, the effect of scan cycle on CV mediated electropolymerisation of octopamine was investigated at 100 mV/s, constant scan rate. The cyclic voltammogram from all cycles showed an irreversible oxidation, indicated by a single anodic peak potential at around +0.52 V in the first scan cycle and which disappeared from the second scan onward (**Fig. 2A**). The same trend was observed from the CV curves of polytyramine (PTyr) deposition, which was used as a

comparison , except that the anodic peak potential was slightly more negative at +0.45 V. Additionally, the impedance data (**Fig. 2B)** showed that the sensors became highly capacitive and resistive as the scan cycle exceeded two cycles. In parallel, the CV of POct-modified electrodes recorded in redox mediator (**Fig. 2C**) showed a significant decrease in current when the scan cycle increased. The electrodes became more insulated as the POct layers form, leading to a lack of electron transfer and stopping the electropolymerisation, thus forming a self-limiting growth of the POct film. No redox waveforms were observed from the POct-modified electrodes compared to the bare gold electrode. These data indicate that a thin POct polymer film with low resistance (137.5 kΩ), compared to the bare DS gold electrode (26.6 kΩ), successfully passivated the electrode surface. This is in agreement with other polyphenol derivatives which form non-conducting polymer layers when electrodeposited onto the sensor surface (Goode et al., 2016; Stejskal, 2015; Tucceri, 2013).

Further optimisation was carried out to determine the effect of scan rates during deposition of POct; it was apparent from the linear plot that the anodic peak current increased proportionally as the scan rate increased (**Fig. 2D and S1**) while the impedance was inversely proportional to the scan rates (**Fig. 2E**) and increasing the scan rate resulted in decreased impedance. The same trends were also observed with deposition of PTyr. All scan rates showed a semi-circular Nyquist plots, indicating that the modified surface was not overly insulating and permeable towards redox mediator.

When probed by surface labelling the chemiluminescence data corroborated with the CV and impedance data showing that the electropolymerisation of octopamine in phosphate buffer at nearly pH 7.5 generated an abundance of surface amines (**Fig. 2F**). Interestingly, the polymer features of POct film developed from a low concentration of octopamine monomer were similar to previous reports in which a polytyramine film was prepared at higher concentrations in alkaline medium (Ahmed et al., 2013; Goode et al., 2016). Finally, several consecutive impedance scans also demonstrated that POct exhibited excellent stability (**Fig. S1**). Together these results i ndicate that electropolymerisation of POct with 2 scan cycles at 100 mV/s scan rate producing an optimal impedance response without completely removing the conductivity.

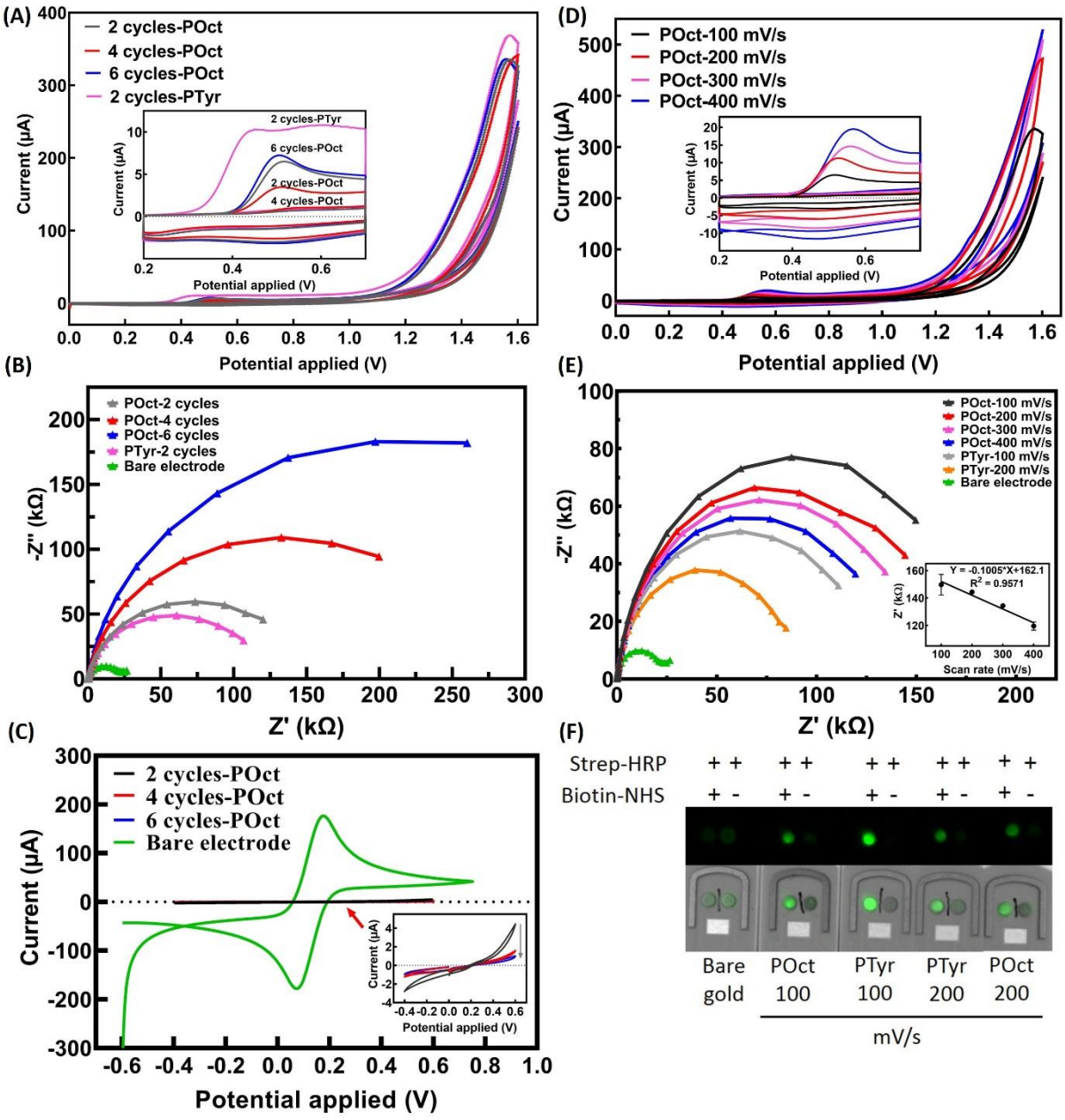

Fig. 2: Electrochemical characterization of POct deposition

(A) CV of POct deposition from varies scan cycles at a constant scan rate of 100 mV/s from 0 to +1.6 V. PTyr was deposited for 2 cycles using the same scan setting as a comparison model. Inset is the enlarged CVs from 0.2V to 0.7 V; (B), Corresponding impedance data and (C), CVs of the electrodeposited polymers in 5 mM $[Fe(CN)_6]^{3-/4-}$ in 100 mM PBS pH 7.1; (D), CVs and (E), EIS scans for POct and PTyr deposition at100-400 mV/s for 2 cycles in 100 mM phosphate buffer, pH 7.5. Inset showing inverse linear relationship between impedance and scan rate for POct deposition; (F), on-sensor blotting on electrodes coated with POct and PTyr at scan rate of 100 mV/s and 200 mV/s for 2 scan cycles. The working electrodes (WE) were incubated with (left WE) and without (right WE) biotin-NHS after polymer deposition. Bare gold screen printed electrodes were included as control. Top panels show pseudo-green captured images, whilst bottom panels superimpose electrode image and pseudo-green image.

3.2. Impedimetric measurement of CEA in buffer

To evaluate the versatility of POct as an amine-functionalised base layer in the fabrication of impedimetric biosensors, monoclonal and polyclonal anti-CEA antibodies were used, representing a large bioreceptor (Mr 150 kDa) whilst Affimers were used as a small bioreceptor (Mr~12.6 kDa). The CEA immunosensors along with a control sensor using anti-digoxin IgG, were fabricated via direct covalent linkage of oxidised oligosaccharide on the Fc region to the POct-modified transducer layer. IgG contains two glycosylation sites located on the heavy chain on the Fc domain. Hence, oxidation of the oligosaccharide moieties should generate an average of two sites containing a reactive aldehyde group per IgG (Wolfe and Hage, 1995). Meanwhile, an alternative affinity binding protein, Affimer (12-14 kDa), which represents the small bioreceptor model was used to fabricate biosensors using indirect conjugation. Thiolated-Affimer was covalently tethered to the POct polymer base layer via the heterobifunctional crosslinker (i.e sulfo-SMCC). Several optimisations have been performed in fabricating the CEA immunosensors and Affimer-based sensor (Fig. S2-3) and optimum results are presented here. In this study, each circuit component present in t**he Randl**e's equivalent circuit (**Fig. S4**), which was used for the curve-fitting of the measured EIS data, was evaluated. A comparative analysis (**Fig. S4**) indicated that R_{CT} was more sensitive and reproducible compared to analyses using capacitance (CPE), phase angle and total impedance (|Z|). Hence, the change in R_{CT} was selected for analysing the response of the biosensors.

In general, increases in impedance were observed in the fully fabricated CEA immunosensors and Affimer-based biosensor (ranging from 45 to 117 kΩ) compared to the bare gold electrode (26.6 kΩ) (**Fig. S5**). Whilst the impedance was reduced when CEA was bound onto the biosensors surface. As can be seen from **Fig. 3 A-B and S6**, site-directed immobilisation of oxidised antibodies onto POct-modified electrode surface yielded highly sensitive and specific CEA biosensors with a limit of detection (LOD) at 9.08 fM and 10.8 fM for the polyclonal and monoclonal-based sensors, respectively. Close proximity of the immune complex antibody-antigen interaction to the transducer surface markedly enhanced the sensitivity of CEA detection. The polyclonal antibody (pAb)-based biosensor showed better performance than the biosensor using a monoclonal antibody (mAb) as bioreceptor; whilst the polyclonal-based sensor had a detection range of 1 fM - 100 nM and its monoclonal equivalent's range was 100 fM - 1 nM. This accords with the mAb recognising a single epitope leading to a narrow detection range. These immunosensors showed good reproducibility towards detection of CEA with the relative standard deviation (RSD) values for the polyclonal and monoclonal based biosensors are 3.81 and 2.55%, respectively. Saturated signal observed at the highest analyte concentration was most probably due to the limited availability of free antibodies for

binding. This immobilisation approach oriented the anchored antibodies in such way that favoured CEA interaction. In addition, the antigen binding sites remained active and were not affected by periodate oxidation. It is important to note that post-functionalisation with the antibodies generated an anti-fouling effect and no surface activation was required prior to the immobilisation step. Blocking steps were not needed as non-specific binding was minimal during CEA interrogation. In both immunosensors, no shift in the R_{CT} values was detected from the control sensor (**Fig. 3 A-B and S6)** which indicated that the impedance signal observed from the anti-CEA sensors represented specific binding.

In comparison, the anti-CEA Affimer based sensors consistently showed a similar pattern of decreased change in impedance upon analyte binding (**Fig. 3C and S6**) and showed better sensitivity and superior detection range (1fM – 100 fM) compared to its counterpart, the monoclonal anti-CEA immunosensor. The LOD of CEA-Affimer sensor was 11.76 fM with RSD value calculated at 4.33% demonstrated that this sensor had good reproducibility. Interestingly, the sensitivity of the CEA-Affimer sensor was close to the polyclonal-based CEA immunosensor although the detection range was narrower for the former sensor. The small size of the anti-CEA Affimer confers extra benefits by generating more binding sites per unit area for interaction with CEA and allows the binding site to be closer to the transducer surface. This is in agreement with Ko Ferrigno (2016) and explains the ultra-sensitive detection observed from the anti-CEA Affimer based biosensor compared to the monoclonal anti-CEA immunosensor. Apart from the bioreceptor size, the thin film of POct on the modified gold electrode also contributed to the improved sensitivity. The thin film of POct enabled the bioreceptors to be located close to the electrode itself which would promote rapid charge transfer to the electrode interface. In the impedimetric biosensor principle, the thin transducer surface generates faster charge transfer from the electrolyte solution to the transducer interface. This leads to a higher sensitivity of detection. Hence, combination of these two factors (i.e. the thin film and small size of Affimer) has substantially enhanced the sensitivity of the proposed CEA biosensors. Decreased resistance observed upon analyte binding in all fabricated CEA biosensors could be due to the POct polymer layer becoming distorted during the binding. This may lead to a pinhole effect, hence accelerating the charge transfer to the electrode interface.

Unlike the CEA immunosensors, Affimer sensors were prone to non-specific interactions and required an additional blocking step prior to CEA interrogation. This is a common problem experienced in the majority of protein based assays in biosensors application (Berggren et al., 2001; Seokheun and Junseok, 2010; Zhang and Heller, 2005). However, the non-specific adsorption did not occur with anti-CEA immunosensors, although the same POct base polymer layer was used. A possible explanation for this is that Affimers are several times smaller than antibodies, hence

immobilisation of an Affimer on a POct film is likely to leave free amino groups accessible on the surface. The larger size of the immobilised IgG on the antibody immunosensors, sterically blocked any free amino groups present. It is postulated that the non-specific signal observed was due to electrostatic interactions on the sensor surface with the $–NH_3^+$ groups. This hypothesis is supported since non-specific signals disappeared after blocking with 10 mM PMDA (**Fig. S7B**) which converts each $–NH_3^+$ into three – COO^- groups. CEA is an anionic protein at pH 7.1 and so PMDA treatment of sensor surface after immobilising the Affimer produces an overall negatively charged surface that minimises non-specific interaction with the mostly anionic proteins. The on-sensor chemiluminescence data (**Fig. S7D**) further corroborated this hypothesis. During the optimisation process, it was found that blocking the non-specific interaction using 1% (w/v) BSA solution (**Fig. S7C**) was not suitable for the Affimer-based biosensor construct. Taking these results into consideration, the proposed biosensors using dual SPGEs provides several advantages including inclusion of the internal control sensor that can eliminate the false positive signals and minimises inter-batch variation measurements.

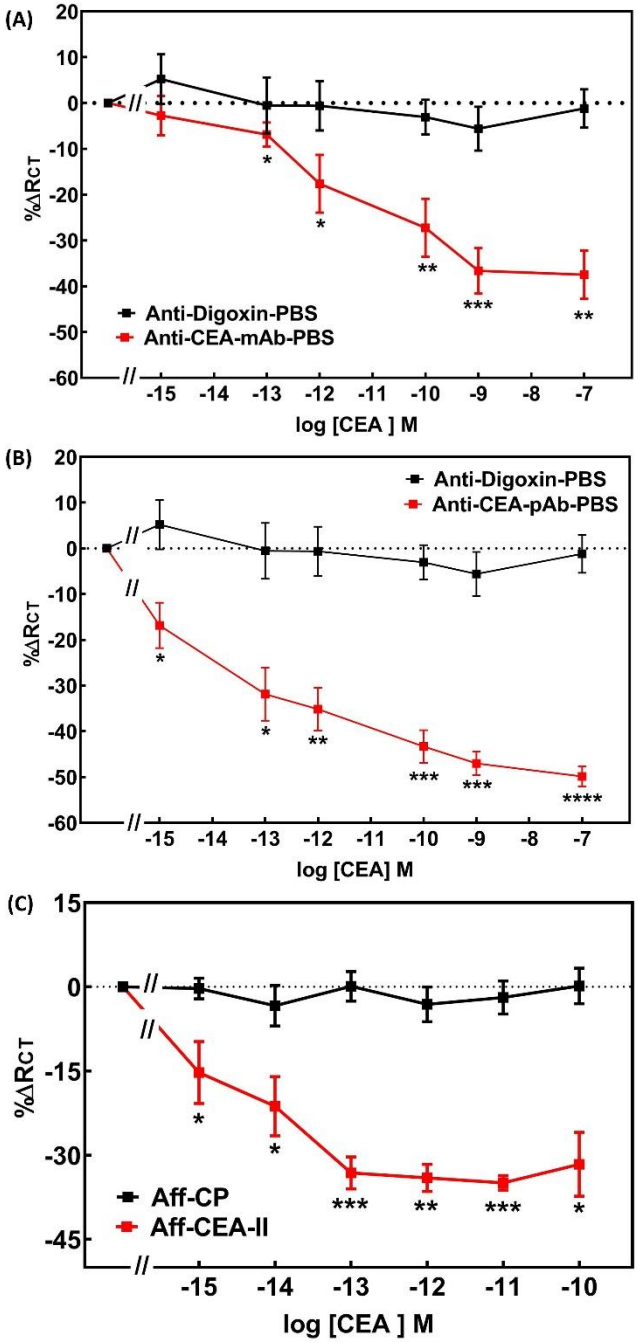

1 **Fig. 3: Impedance profiles of anti-CEA IgG and Affimer based sensors in buffer**

2 Calibration curve of the normalised R_{CT} data from the corresponding immunosensors; (A),
3 monoclonal and (B), polyclonal anti-CEA antibodies and (I), Affimer based biosensors showing the
4 percentage change in R_{CT} (n= 4± SEM). Mean differences between anti-CEA and control sensors
5 were statistically significant by independent t-test (*, **, *** and **** indicate significance at p
6 <0.03, 0.002, 0.0002 and 0.0001, respectively).

7

3.3. Impedimetric measurement for CEA in diluted serum system

As proof of concept, the optimised CEA immunosensors and Affimer based sensor were evaluated in a range of serum dilutions to examine the biosensors' in a biological matrix. The presence of CEA in serum is routinely used in diagnosing CRC (Kim et al., 2009; Su et al., 2012). The EIS measurements were repeated in the same manner as for PBS and included the same control sensors, but this time the CEA solutions were spiked with diluted serum. Fully fabricated CEA sensors were initially tested in the absence of CEA in a series of diluted normal human serum to rule out the non-specific binding from serum diluent. In the CEA immunosensors, 1% (v/v) serum diluted in 10 mM PBS, pH 7.4 showed minimal non-specific binding (**Fig. 4A**). However, for the anti-CEA-Affimer biosensor, further dilutions were needed and 0.001% (v/v) serum revealed the least non-specific binding. R_{CT} measured in the blank serum was used as the baseline sensor. The change in impedance was calculated by subtracting R_{CT} measured in the blank serum from the R_{CT} recorded in each concentration of CEA and then normalised to a percentage change.

It can be clearly seen in **Fig. 4B** that a significant increase in R_{CT} was observed with the anti-CEA pAb immunosensor exposed to CEA solution spiked with 1% (v/v) serum as compared to the control sensor. The lowest level of detection remained at 1 fM though a linear calibration, as in PBS was difficult to attain. In contrast, the change in R_{CT} was reduced by half in the anti-CEA mAb immunosensor. A similar trend was observed in the anti-CEA Affimer based sensor (**Fig. 4C**) where lowest level of CEA detection remained at 1 fM and the maximum detection was at 100 fM.

Interestingly, the change in impedance consistently increased when the sensor was exposed to CEA in serum, whilst a decreasing R_{CT} was seen when the sensor was used in buffer. This further supports the earlier theory of polymer distortion and pinhole effects postulated for the buffered system. However, this time the presence of serum components occupied the empty spaces in between the immobilised antibodies or Affimer. Therefore, upon analyte binding, stretching of the polymer was restricted by the presence of non-specifically bound material that led to an increase in resistance. Non-specific binding observed from the control sensors, anti-digoxin immunosensor and anti-calprotectin Affimer sensor, was negligible which confirmed the specificity of binding of the anti-CEA immunosensors and anti-CEA Affimer sensor. Additionally, it is important to highlight that a substantial non-specific fouling was observed when testing out the proposed sensors in lower dilutions of serums.

Although the serum dilution was high in this study, this may be an advantage. Since when real patient samples are tested, the blood sample would need to be pre-diluted by around 10^5 for CEA as the pathological cut-off value for CEA is clinically set at $\geq$ 5 ng/ml (equivalent to 25 pM) and this

concentration exceeds the detection range of the POct-based biosensors. A 10^5 times dilution would reduce the CEA concentration to 2.5 fM which is well within the detection range. This dilution would also indirectly reduce non-specific binding from serum components and allow the specific signal to be detected.

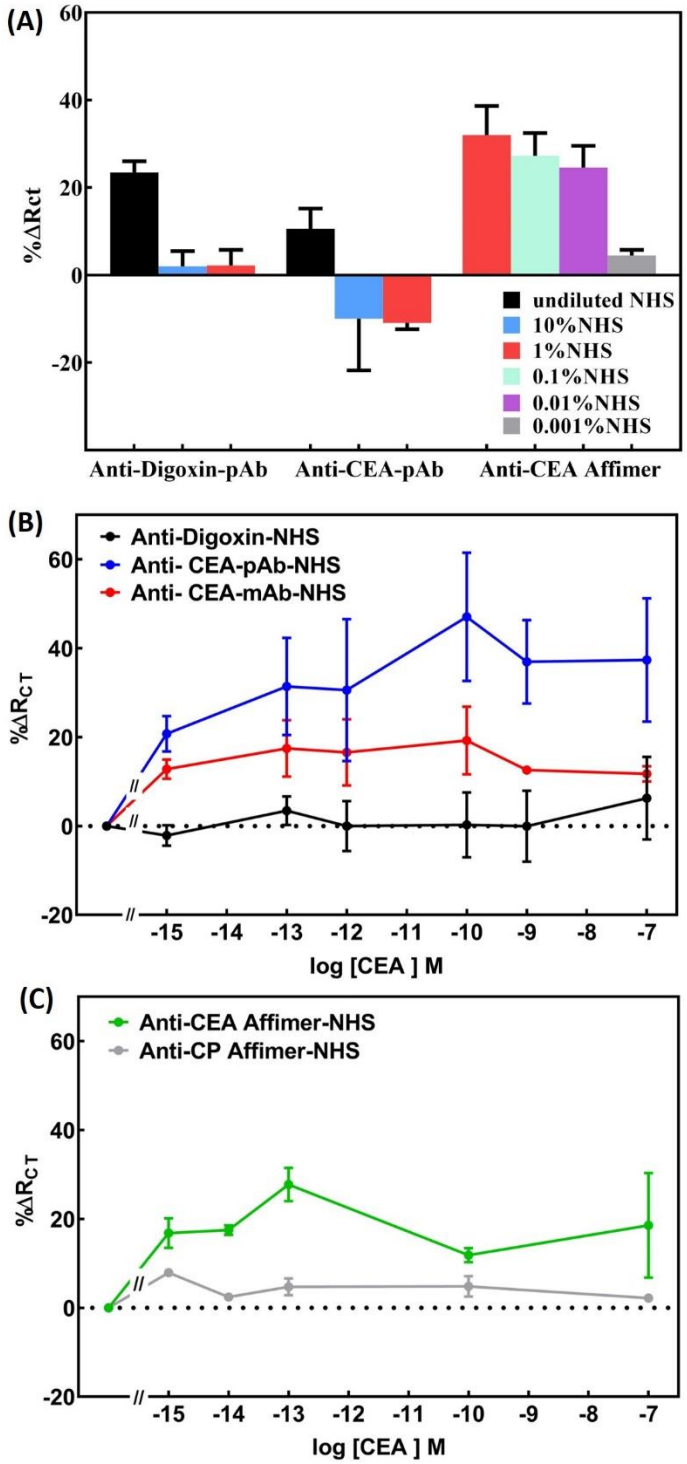

Fig. 4: Comparison of POct based biosensor performance in diluted serum

(A), the optimised immunosensors (pAb anti-CEA IgG and control sensor, pAb anti-digoxin IgG) were tested against undiluted, 10 % (v/v) and 1% (v/v) normal human serum (NHS) diluted in 10 mM PBS, pH 7.4 in the absence of CEA. Similarly, the optimised anti-CEA Affimer biosensor was tested in higher dilutions from 1- 0.001% (v/v) in the absence of CEA. ΔR_{CT} was calculated by subtracting R_{CT} measured in PBS from R_{CT} recorded in diluted serum and normalised. Data are mean ± SEM (n=4). Sensor performance was subsequently tested in CEA spiked in 1% and 0.001% (v/v) diluted human serum for immunosensors and Affimer sensor, respectively; (B), sensors using anti-CEA mAb ( ) or pAb ( ), or anti-digoxin pAb ( ) as bioreceptor; (C), sensors using Affimers against CEA ( ) or calprotectin ( ).

3.4. Comparison of detection range of anti-CEA polyoctopamine-based biosensors with other assays

Comparative analysis between different detection techniques was conducted to evaluate the analytical performance of anti-CEA POct-based impedimetric biosensors developed in this study with commercial ELISA kit and SPR-based assay using Biacore (Shamsuddin et.al, article in press 2021). It can be clearly seen in **Fig. 5** that the POct-based impedimetric biosensors performed with high sensitivity and specificity with a wider detection range compared to the other assays. The Affimer and pAb based biosensors showed the highest sensitivity, followed by mAb based immunosensor, ELISA and SPR. Additionally, the pAb based immunosensor exhibited the widest dynamic detection range compared to the other detection assays. This is almost certainly since the anti-CEA pAb contains many individual clones with low to high affinities and whose binding curves are additive. The anti-CEA Affimer based sensor range could be extended by producing a "synthetic polyclonal" Affimer mix, by combining several Affimer clones of varying affinity. CEA analysis by the ELISA kit showed moderate sensitivity with a limit of detection at 10 pM and dynamic range from 25 to 600 pM. Meanwhile, SPR provided the least sensitive detection with minimal binding observed at 7. 8 nM and dynamic detection range from 7.8 nM to 1µM. Overall, the impedimetric biosensors fabricated using POct as a non-conducting polymer layer produced ultra-sensitive CEA detection and was comparable or better than the published data, summarised in **Table 1**.

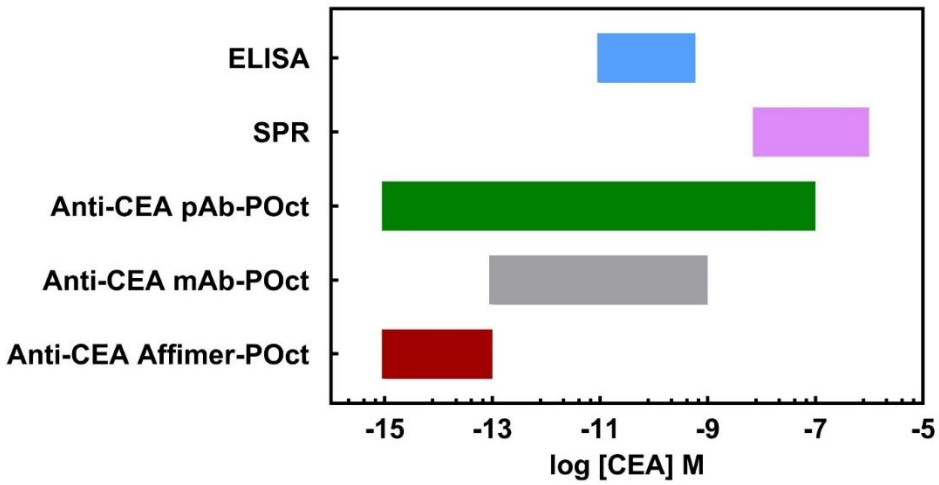

Fig. 5: Comparison between sensitivity and dynamic range of anti-CEA polyoctopamine based biosensors and other assays

The analytical performance of anti-CEA POct-based impedimetric biosensors and other detection assays is shown. The sensitivity and detection range of commercial ELISA kits, SPR assay using Biacore and POCt-based biosensors using pAb, mAb or Affimer as the bioreceptor is shown.

Table 1: Comparison of the analytical performance of electrochemical impedimetric biosensors for CEA detection

Random orientation

Detection	Transducer	Immobilization technique	Bioreceptor	LOD	Reference (s)
Label-free	Gold	Electro-copolymerization of o-aminophenol with CEA-Ab-glutathione monolayer modified AuNP	Antibody	0.1 ng/ml (500 fM)	(Tang et al., 2007)
	Glassy carbon electrode (GCE)	Physisorption of anti-CEA antibody onto GCE modified with AuNP/ polymeric self-assembled nanoparticles (poly (γ-glutamic acid)-dopamine-chitosan	Antibody	10 fg/ml (50 aM)	(Xu et al., 2017)
	Glassy carbon electrode (GCE)	Covalent immobilisation of amine-modified CEA aptamer on GA-AuNP/AMCM-GCE	DNA Aptamer	0.98 pg/ml (4.9 fM)	(Shekari et al., 2017)
	Conducting Whatman paper	Covalent immobilization of anti-CEA antibody onto amine-functionalised surface coated with conducting poly (3,4ethylenedioxythiophene):poly(4-styrene sulfonate) on paper electrode	Antibody	2.68 ng/ml (13.4 pM)	(Kumar et al., 2016)
	Graphite-based screen-printed electrode	Covalent immobilization of anti-CEA antibody onto poly-(pyrrole-3-carboxylic acid)-modified electrode	Antibody	33.33 pg/ml (166.65 fM)	(Iordănescu et al., 2018)
Labelled	Indium tin oxide (ITO) electrode on a glass slide	Covalent immobilization of anti-CEA antibody onto aldehyde-functionalised ITO electrode and sandwich with magnetic beads coated with secondary antibody for signal enhancement	Antibody	1 ng/ml (5 pM)	(Yeh et al., 2016)
	Glassy carbon electrode (GCE)	Covalent immobilization of anti-CEA antibody onto AuNP-modified GCE and sandwich with HRP conjugated to secondary antibody functionalised with graphene oxide nanosheets and coupled with enzymatic biocatalytic precipitation of 4-chloro-1-naphthol	Antibody	0.64 pg/ml (3.2 fM)	(Hou et al., 2013)
Site-directed orientation					
Label-free	Screen printed gold electrode (SPGE)	Covalent immobilization of anti-CEA antibodies onto electropolymerised polyoctopamine coated SPGE	Monoclonal antibody	2.16 pg/ml (10.8 fM)	This study
			Polyclonal antibody	1.82 pg/ml (9.08 fM)	
	Screen printed gold electrode (SPGE)	Covalent immobilization of anti-CEA Affimer onto electropolymerised polyoctopamine coated SPGE	Affimer	2.35 pg/ml (11.76 fM)	This study

4. Conclusions

This study has demonstrated the potential of a novel polyoctopamine film and proposed to be utilized as an alternative non-conducting transducer base layer for amine-functionalisation in electrochemical biosensor applications. Here, we showed the POct polymer layer provides a versatile functionalisation technique to immobilise a variety of bioreceptors including large bioreceptors (e.g. antibodies) and small bioreceptors (e.g. Affimers). The thin film formed by POct on the gold electrode enhanced the sensitivity of CEA detection down to fM levels without the requirement for signal amplification that is normally needed in labelled detection bioassays. Additionally, this study also demonstrated the use of Affimer as alternative bioreceptor to target CEA that showed remarkable sensitivity and specificity as compared to the anti-CEA immunosensors and can be considered a practical replacement for the mAb as bioreceptor. Overall, the proposed CEA biosensors fabricated in this study offer rapid response times (less than 5 min), use of small sample volumes (10 µl), simple fabrication techniques with the incorporation of internal control sensor that can eliminate the false positive signals and minimises inter-batch variation measurements. Ultimately, findings in this study supports for the development of POC biosensor devices as a CRC diagnostic tool. Further work is proposed to expand the narrow range of detection due to the small size of working electrode area. This can be improved by incorporating the nanomaterial onto the transducer layer that can increase the binding surfaces to immobilise the Affimers or monoclonal antibody; hence improve the accessibility for the CEA binding, which could enhance the biosensor performance.

CRediT authorship contribution statement

Shazana Hilda Shamsuddin: Conceptualization, Methodology, Validation, Formal analysis, Investigation, Writing - original draft, Funding acquisition. Timothy D. Gibson: Methodology, Formal analysis, Resources, Writing - Review & Editing. Darren C. Tomlinson: Resources, Supervision. Michael J. McPherson: Resources, Writing - Review & Editing, Supervision. David G. Jayne: Resources, Supervision. Paul A. Millner: Conceptualization, Methodology, Validation, Resources, Writing - Review & Editing, Supervision.

Acknowledgements: The authors acknowledge and thank the Universiti Sains Malaysia (USM) and Ministry of Higher Education Malaysia for funding this research project. We also thank the BioScreening and Technology group (BSTG) for the phage display facilities and assistances, and Dr. Iain Manfield for the excellent technical support in SPR assay analysis, and the Wellcome Trust grant (062164/Z/00/Z) for funding the BIACORE3000 instrument, and Dr. Jack Goode, Mr. Duncan Sharp and Mr. Juan Leva Bueno for the technical assistance in electrochemical analysis. Thanks also go to Dr. Mohd Zulkifli Mustafa for editorial assistance.

References:

Adamson, H., Ajayi, M.O., Campbell, E., Brachi, E., Tiede, C., Tang, A.A., Adams, T.L., Ford, R., Davidson, A., Johnson, M., McPherson, M.J., Tomlinson, D.C. & Jeuken, L.J.C., 2019. ACS Sensors 4(11), pp.3014-3022.

Ahmed, A.,2015. PhD, University of Leeds.

Ahmed, A., Rushworth, J.V., Wright, J.D. & Millner, P.A., 2013. Anal Chem 85(24), pp.12118-12125.

Armbruster, D.A. & Pry, T., 2008. The Clinical biochemist. Reviews 29 Suppl 1(Suppl 1), pp.S49-S52.

Arnold, M., Sierra, M.S., Laversanne, M., Soerjomataram, I., Jemal, A. & Bray, F., 2017. Gut 66(4), pp.683-691.

Beauchemin, N. & Arabzadeh, A., 2013. Cancer and Metastasis Reviews 32(3-4), pp.643-671.

Berggren, C., Bjarnason, B. & Johansson, G., 2001. Electroanalysis 13(3), pp.173-180.

Cosnier, S. & Holzinger, M., 2011. Chemical Society Reviews 40(5), pp.2146-2156.

Gibson, T.D. & Sharp, D.W.M., 2017. Electrochemical Biosensors, EP 3246698B1, Great Britain, pp. 15.

Gomes, R.S., Moreira, F.T., Fernandes, R. & Sales, M.G.F., 2018. PloS one 13(5), pp.e0196656.

Goode, J., Dillon, G. & Millner, P.A., 2016. Sensors and Actuators B: Chemical 234, pp.478-484.

Goode, J.A.,2015. PhD, University of Leeds.

Hammond, Jules L., Formisano, N., Estrela, P., Carrara, S. & Tkac, J., 2016. Essays in Biochemistry 60(1), pp.69-80.

Hou, L., Cui, Y., Xu, M., Gao, Z., Huang, J. & Tang, D., 2013. Biosensors and Bioelectronics 47, pp.149-156.

Huang, J.-Y., Zhao, L., Lei, W., Wen, W., Wang, Y.-J., Bao, T., Xiong, H.-Y., Zhang, X.-H. & Wang, S.-F., 2018. Biosensors and Bioelectronics 99, pp.28-33.

Iordănescu, A., Tertis, M., Cernat, A., Suciu, M., Săndulescu, R. & Cristea, C., 2018. Electroanalysis 30(6), pp.1100-1106.

Ismail, F. & Adeloju, S.B., 2010. Sensors 10(4), pp.2851-2868.

Jeuken, L.J.C., 2016. Adv Biochem Eng Biotechnol 158, pp.43-73.

Kim, J.Y., Kim, N.K., Sohn, S.K., Kim, Y.W., Kim, K.J., Hur, H., Min, B.S. & Cho, C.H., 2009. Ann Surg Oncol 16(10), pp.2771-2778.

Ko Ferrigno, P., 2016. Essays In Biochemistry 60(1), pp.19-25.

Koutsoumpeli, E., Tiede, C., Murray, J., Tang, A., Bon, R.S., Tomlinson, D.C. & Johnson, S., 2017. Analytical Chemistry 89(5), pp.3051-3058.

Kumar, S., Kumar, S., Pandey, C.M. & Malhotra, B.D., 2016. Journal of Physics: Conference Series 704(1), pp.012010.

Labianca, R., Nordlinger, B., Beretta, G.D., Brouquet, A., Cervantes, A. & Group, E.G.W., 2010. Ann Oncol 21 Suppl 5, pp.v70-77.

Liu, Z. & Ma, Z., 2013. Biosensors and Bioelectronics 46, pp.1-7.

Lv, H., Li, Y., Zhang, X., Gao, Z., Zhang, C., Zhang, S. & Dong, Y., 2018. Biosensors and Bioelectronics 112, pp.1-7.

Pinyou, P., Blay, V., Muresan, L.M. & Noguer, T., 2019. Materials Horizons 6(7), pp.1336-1358.

Rushworth, J., Ahmed, A. & Millner, P., 2013a. J Biosens Bioelectron 4, pp.146.

Rushworth, J.V., Hirst, N.A., Goode, J.A., Pike, D.J., Ahmed, A. & Millner, P.A., 2013b. Impedimetric biosensors for medical applications current progress and challenges, ASME Press, New York.

Seokheun, C. & Junseok, C., 2010. Journal of Micromechanics and Microengineering 20(7), pp.075015.

Sharma, R., Deacon, S.E., Nowak, D., George, S.E., Szymonik, M.P., Tang, A.A.S., Tomlinson, D.C., Davies, A.G., McPherson, M.J. & Wälti, C., 2016. Biosensors and Bioelectronics 80, pp.607-613.

Shamsuddin, S.H., Jayne, D.G., Tomlinson, D.C., McPherson, M.J. & Millner, P.A., 2021. Scientific Reports, pp.1-10.

Shekari, Z., Zare, H.R. & Falahati, A., 2017. Journal of The Electrochemical Society 164(13), pp.B739-B745.

Stejskal, J., 2015. Progress in Polymer Science 41, pp.1-31.

Su, B.B., Shi, H. & Wan, J., 2012. World J Gastroenterol 18(17), pp.2121-2126.

Sun, X., Hui, N. & Luo, X., 2017. Microchimica Acta 184(3), pp.889-896.

Tang, H., Chen, J., Nie, L., Kuang, Y. & Yao, S., 2007. Biosensors and Bioelectronics 22(6), pp.1061-1067.

Thangsunan, P., Lal, N., Tiede, C., Moul, S., Robinson, J.I., Knowles, M.A., Stockley, P.G., Beales, P.A., Tomlinson, D.C., McPherson, M.J. & Millner, P.A., 2021. Sensors and Actuators B: Chemical 326, pp.128829.

Thévenot, D.R., Toth, K., Durst, R.A. & Wilson, G.S., 2001. Biosensors and Bioelectronics 16(1), pp.121-131.

Tiede, C., Bedford, R., Heseltine, S.J., Smith, G., Wijetunga, I., Ross, R., AlQallaf, D., Roberts, A.P.E., Balls, A., Curd, A., Hughes, R.E., Martin, H., Needham, S.R., Zanetti-Domingues, L.C., Sadigh, Y., Peacock, T.P., Tang, A.A., Gibson, N., Kyle, H., Platt, G.W., Ingram, N., Taylor, T., Coletta, L.P., Manfield, I., Knowles, M., Bell, S., Esteves, F., Maqbool, A., Prasad, R.K., Drinkhill, M., Bon, R.S., Patel, V., Goodchild, S.A., Martin-Fernandez, M., Owens, R.J., Nettleship, J.E., Webb, M.E., Harrison, M., Lippiat, J.D., Ponnambalam, S., Peckham, M., Smith, A., Ferrigno, P.K., Johnson, M., McPherson, M.J. & Tomlinson, D.C., 2017. eLife 6, pp.e24903.

Tiede, C., Tang, A.A.S., Deacon, S.E., Mandal, U., Nettleship, J.E., Owen, R.L., George, S.E., Harrison, D.J., Owens, R.J., Tomlinson, D.C. & McPherson, M.J., 2014. Protein Engineering Design & Selection 27(5), pp.145-155.

Tucceri, R., 2013. American Journal of Analytical Chemistry 4, pp.13-26.

Turner, A.P., 2013. Chem Soc Rev 42(8), pp.3184-3196.

Wolfe, C.A. & Hage, D.S., 1995. Analytical biochemistry 231(1), pp.123-130.

Wu, X.-Z., Ma, F. & Wang, X.-L., 2010. World journal of gastroenterology: WJG 16(32), pp.4084.

Xu, S., Zhang, R., Zhao, W., Zhu, Y., Wei, W., Liu, X. & Luo, J., 2017. Biosensors and Bioelectronics 92, pp.570-576.

Yarman, A., Turner, A. & Scheller, F., 2014. Electropolymers for (nano-) imprinted biomimetic biosensors, in, Nanosensors for chemical and biological applications. Elsevier, pp 125-149.

Yeh, C.-H., Su, K.-F. & Lin, Y.-C., 2016. Sensors and Actuators A: Physical 241, pp.203-211.

Yuqing, M., Jianrong, C. & Xiaohua, W., 2004. Trends Biotechnol 22(5), pp.227-231.

Zhang, Y. & Heller, A., 2005. Analytical Chemistry 77(23), pp.7758-7762.

Zhurauski, P., Arya, S.K., Jolly, P., Tiede, C., Tomlinson, D.C., Ko Ferrigno, P. & Estrela, P., 2018. Biosensors and Bioelectronics 108, pp.1-8.

Title: Reagentless Affimer- and antibody-based impedimetric biosensors for CEA-detection using a novel non-conducting polymer

Shazana Hilda Shamsuddin[a,b,*], Timothy D. Gibson[a], Darren C. Tomlinson[c], Michael J. McPherson[c], David G. Jayne[d], Paul A. Millner[a]**

[a] The Leeds Bionanotechnology Group, School of Biomedical Sciences, University of Leeds, LS2 9JT, Leeds, United Kingdom
[b] Department of Pathology, School of Medical Sciences, Health Campus, Universiti Sains Malaysia, 16150, Kelantan, Malaysia
[c] Astbury Centre for Structural and Molecular Biology, University of Leeds, LS2 9JT, Leeds, United Kingdom
[d] Leeds Institute of Medical Research, University of Leeds, LS9 7TF, Leeds, United Kingdom

Correspondence and requests for materials should be addressed to [*]S.H.S. (email: shazana.hilda@usm.my) or [**]P.A.M. (email: P.A.Millner@leeds.ac.uk)

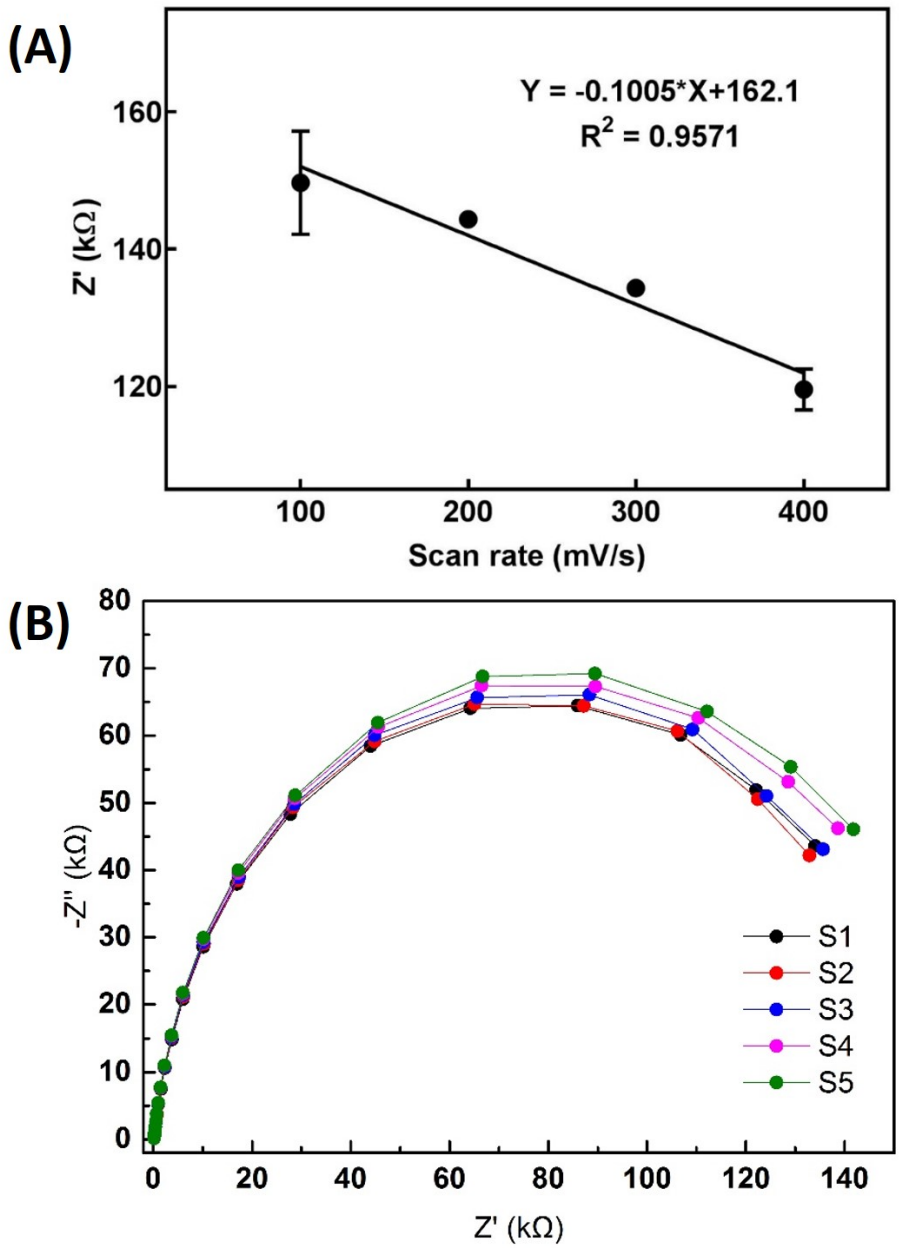

Fig. S1: Electrochemical characterization of POct deposition

(A) Linear relationship between anodic peak current and scan rate for POct deposition; (C), Nyquist plots of five consecutive impedance scans on POct film in 10 mM $[Fe(CN)_6]^{3-/4-}$.

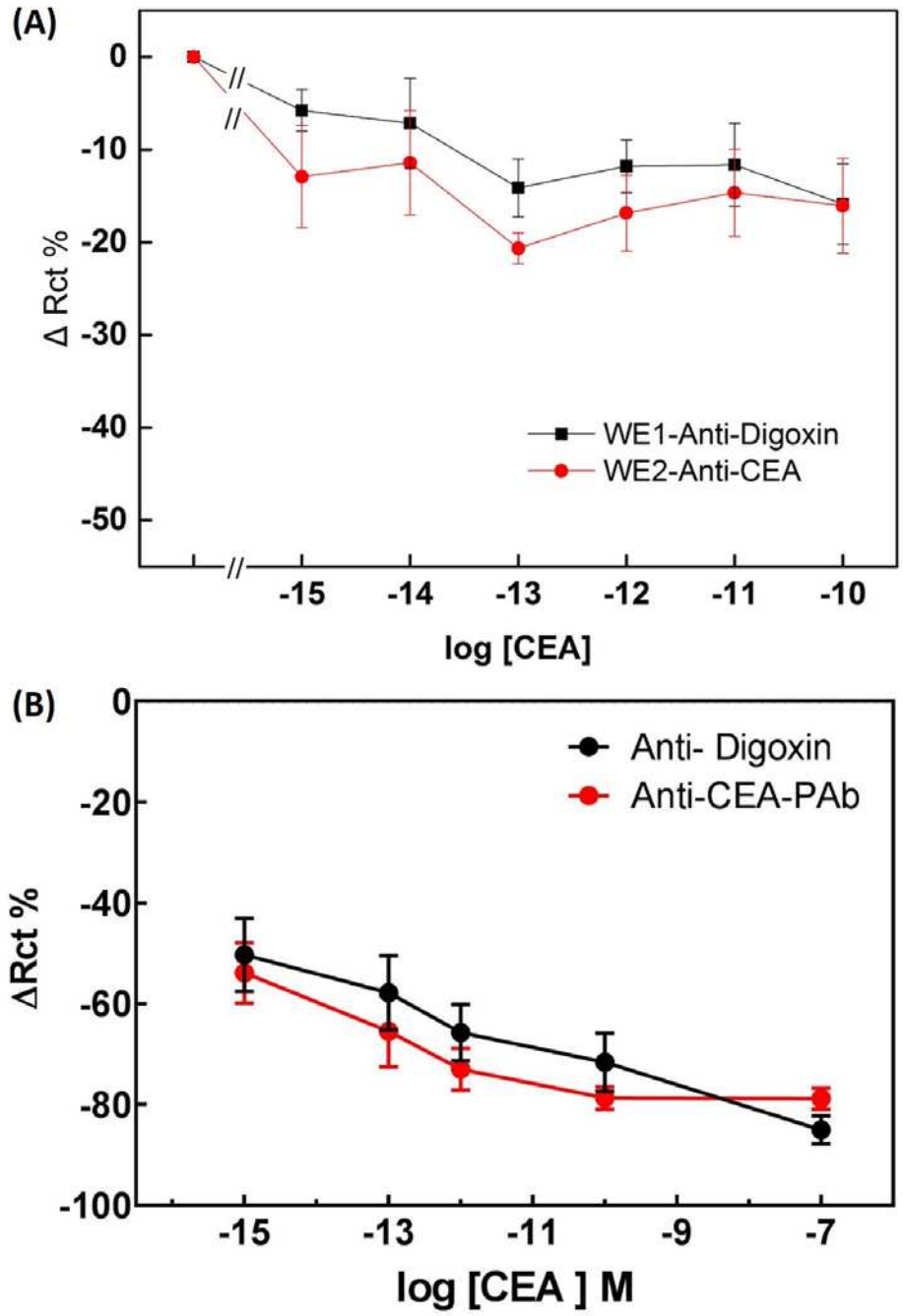

Fig. S2: Optimisation of the CEA immunosensors fabrication

Impedance data of the CEA immunosensors fabricated based on (A) antibody entrapment via electropolymerisation of octopamine and $MS(PEG)_4$ conjugate; and (B) electropolymerisation of oxidised antibodies conjugated to POct. The calibration curve of corresponding immunosensors plotted as normalised data showing the percentage change in R_{CT} (n= 4± SEM). EIS was recorded in 10 mM [Fe(CN)6]3-/4- in 100 mM PBS pH 7.1. All biosensors construct showing non-specific binding on both positive and control sensors.

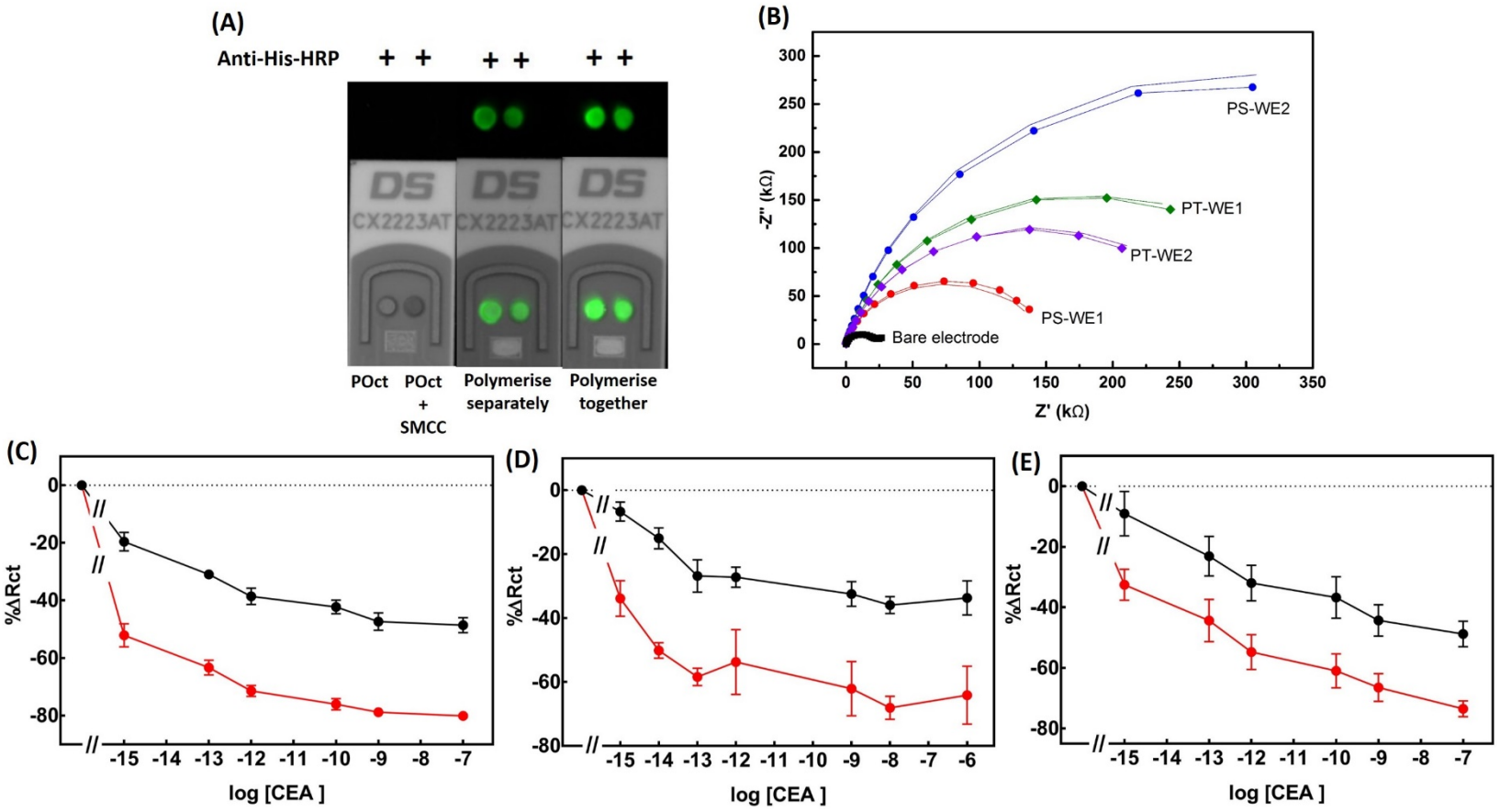

Fig. S3: Optimisation of the CEA-Affimer biosensor fabrication

Impedance data showing the optimisation on (A, B) the effect of different immobilisation techniques; and determination of the CEA-Affimer concentration on sensor surface (C), 3.96 µM (D), 7.92 µM and (E) 15.84 µM alongside with the control sensor, anti-calprotectin-Affimer. All biosensors construct showing non-specific binding on both positive and control sensors. CEA binding was interrogated in cumulative fashion from 1 fM to 1 µM (n = 5± SEM).

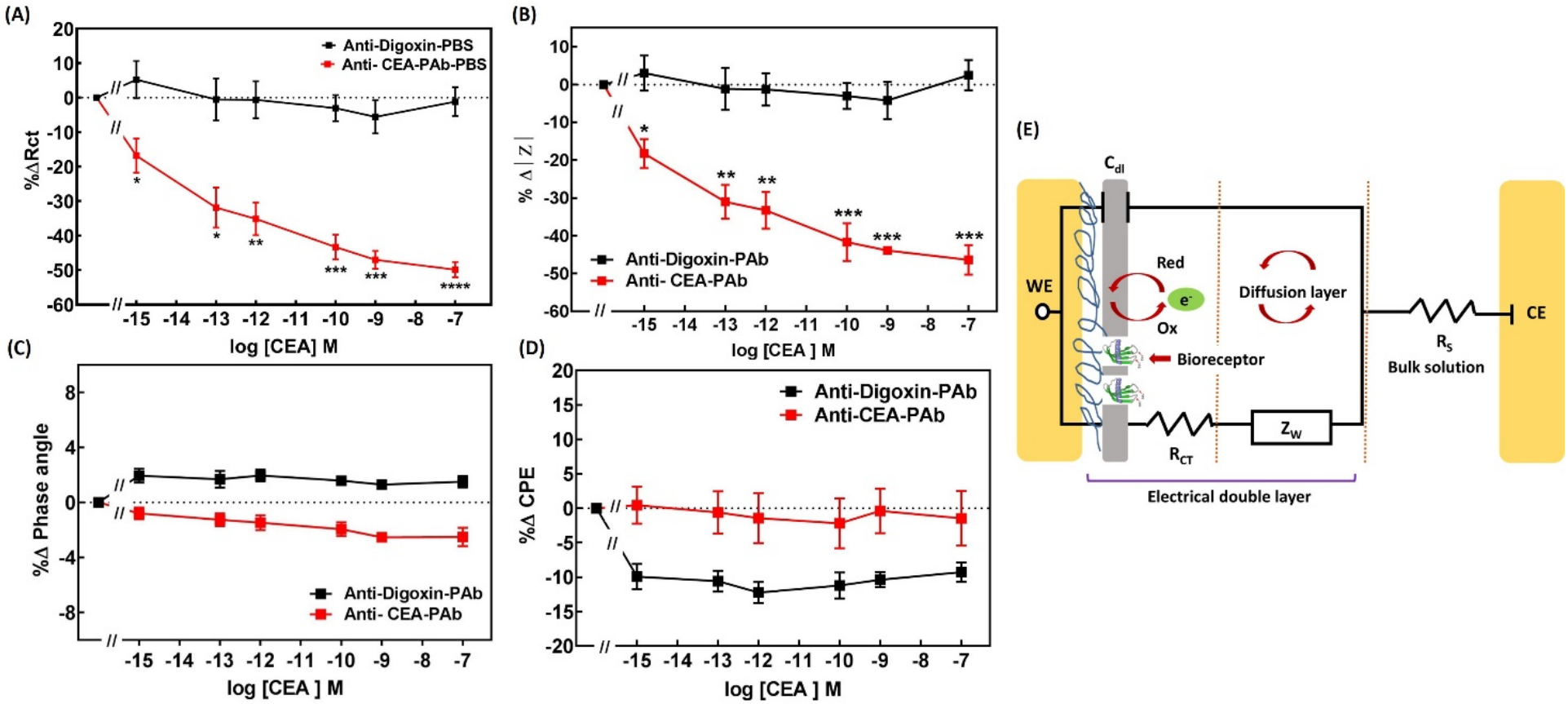

Fig. S4: Comparative analysis of impedance measurements derived from the Randle's equivalent circuit

Calibration curves of normalised data from ( ), anti-CEA and ( ), anti-digoxin pAb based sensors showing Δ% in (A), R_{CT}; (B), total impedance (|Z|) at 0.25 Hz; (C), phase angle at 53.86 Hz where the maximum change observed and (D), capacitance. EIS measurements were from 2.5 KHz to 250 mHz and EIS fitting were using the Randle's equivalent circuit as shown in (E). Data are means ±SEM (n= 4). Statistical significant was determined by independent t-test and *, **, *** and **** indicate significance with p-value <0.03, 0.002, 0.0002 and 0.0001, respectively).

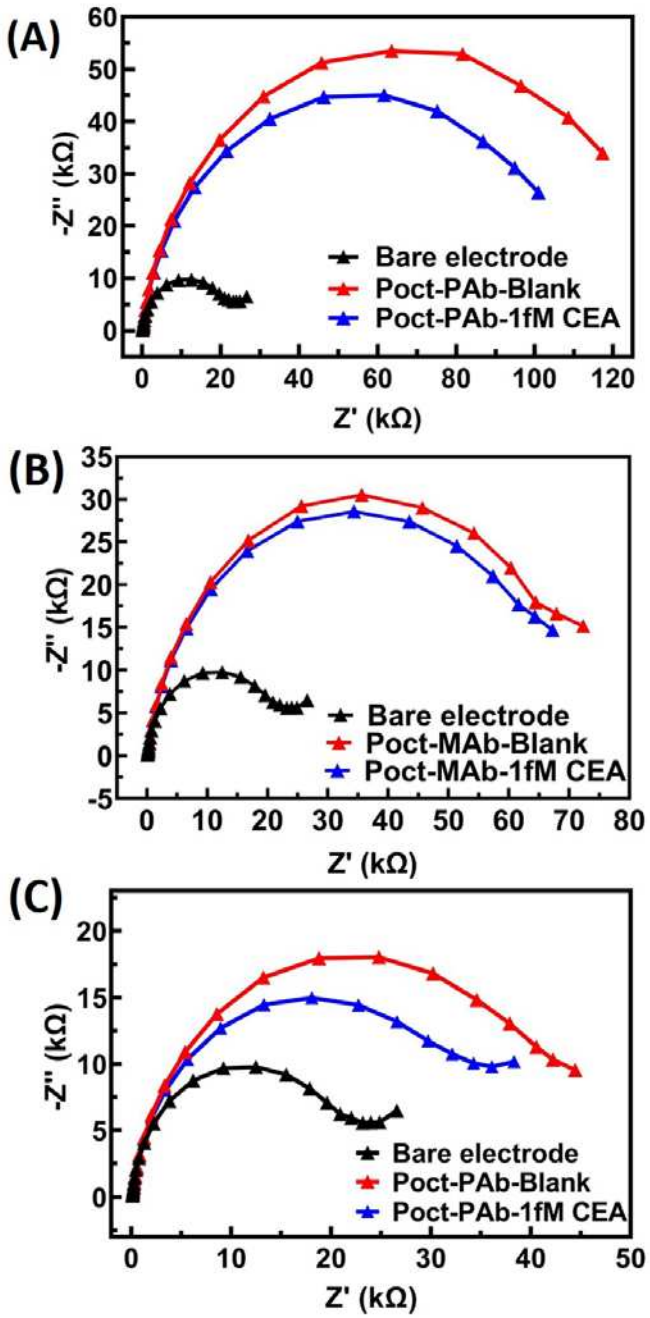

Fig. S5: Fabrication of POct-based biosensors

Nyquist plots showing the fabrication of (A), polyclonal-based and (B), monoclonal-based immunosensors; and (C), Affimer-based biosensor for CEA detection. The impedance of fully constructed CEA biosensors (★) were initially increased compared to the bare gold electrode (★) and decreased when binding specifically to CEA (★).

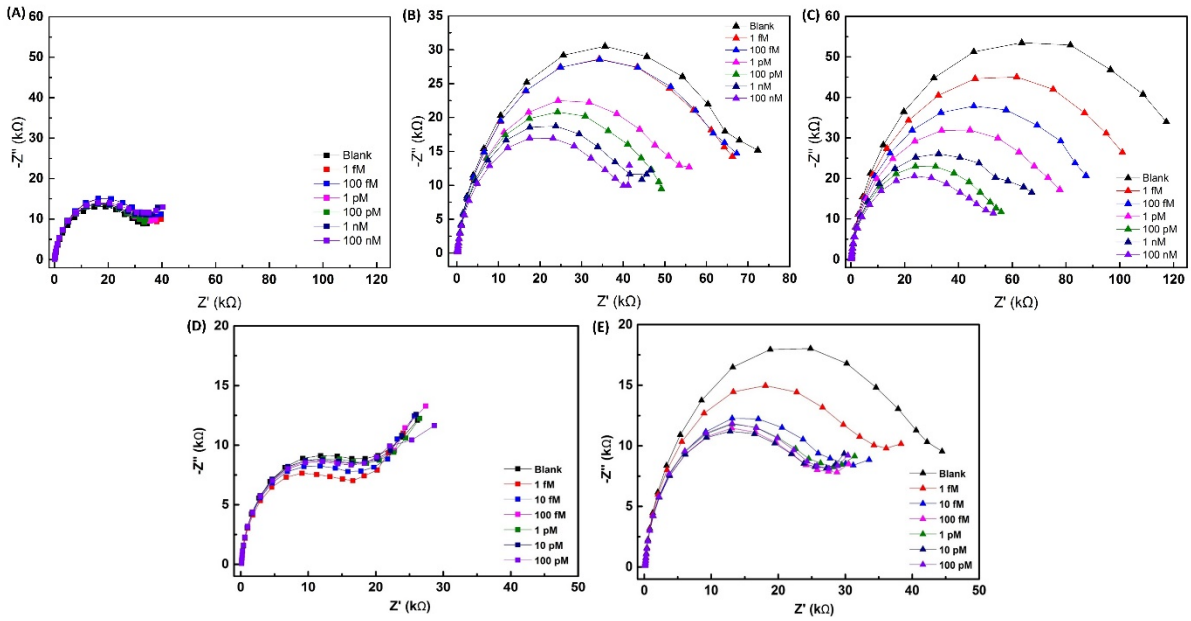

Fig. S6: Impedance profiles of anti-CEA IgG and Affimer based sensors in buffer

Nyquist plots showing impedance signals when increasing concentration of CEA (from 1 fM to 100 nM) cumulatively incubated on (A), anti-digoxin polyclonal antibody; (B, C) anti-CEA monoclonal and polyclonal antibody-based sensors, respectively; (D, E), anti-calprotectin and anti-CEA Affimer-based sensors, respectively.

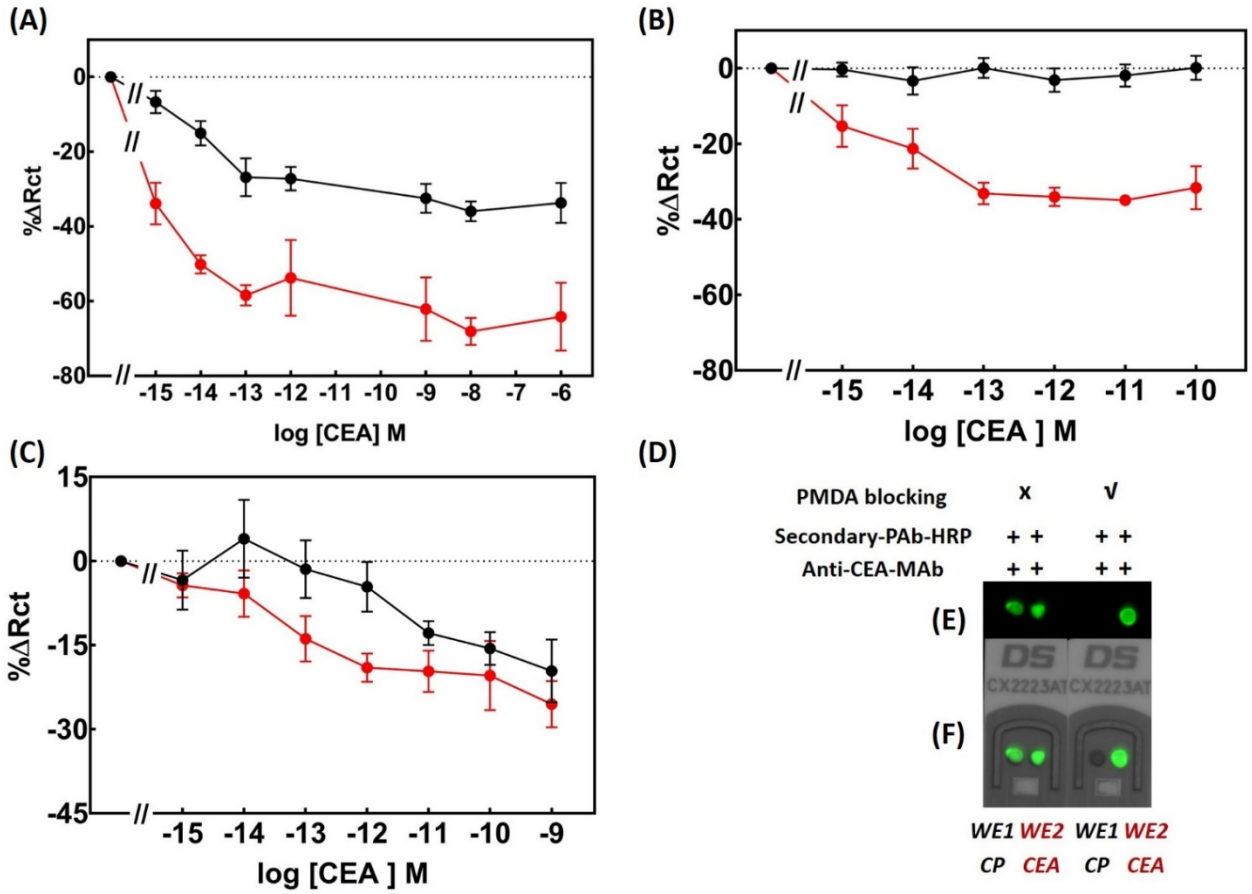

Fig. S7: CEA recognition by Affimer based sensors under different blocking conditions

Sensors were exposed to CEA under the following conditions: (A), without blocking; (B) after blocking with 10 mM PMDA solution and (C), blocking with 1% (w/v) BSA. Specific and non-specific biosensors were constructed using anti-CEA Affimer, (—●—) and anti-calprotectin (CP) Affimer, ( ) respectively. (D) On-sensor blotting after addition of 1pM of CEA showing sensors blocked with 10 mM PMDA (right panel). The pseudo-green colour on specific sensor (WE2-CEA, right panel) shows specific CEA binding whilst non-blocked sensors on the left show non-specific binding of CEA or CP on the sensor surface. (E), the top panels show pseudo-green colouring of the captured images, which (F), are superimposed on the images of the electrodes.

Title: Reagentless Affimer- and antibody-based impedimetric biosensors for CEA-detection using a novel non-conducting polymer

Shazana Hilda Shamsuddin[a,b,*], Timothy D. Gibson[a], Darren C. Tomlinson[c], Michael J. McPherson[c], David G. Jayne[d], Paul A. Millner[a]**

[a] The Leeds Bionanotechnology Group, School of Biomedical Sciences, University of Leeds, LS2 9JT, Leeds, United Kingdom
[b] Department of Pathology, School of Medical Sciences, Health Campus, Universiti Sains Malaysia, 16150, Kelantan, Malaysia
[c] Astbury Centre for Structural and Molecular Biology, University of Leeds, LS2 9JT, Leeds, United Kingdom
[d] Leeds Institute of Medical Research, University of Leeds, LS9 7TF, Leeds, United Kingdom

Correspondence and requests for materials should be addressed to [*]S.H.S. (email: shazana.hilda@usm.my) or [**]P.A.M. (email: P.A.Millner@leeds.ac.uk)

CRediT authorship contribution statement

Shazana Hilda Shamsuddin: Conceptualization, Methodology, Validation, Formal analysis, Investigation, Writing - original draft, Funding acquisition. Timothy D. Gibson: Methodology, Formal analysis, Resources, Writing - Review & Editing. Darren C. Tomlinson: Resources, Supervision. Michael J. McPherson: Resources, Writing - Review & Editing, Supervision. David G. Jayne: Resources, Supervision. Paul A. Millner: Conceptualization, Methodology, Validation, Resources, Writing - Review & Editing, Supervision.

Acknowledgements: The authors acknowledge and thank the Universiti Sains Malaysia (USM) and Ministry of Higher Education Malaysia for funding this research project. We also thank the BioScreening and Technology group (BSTG) for the phage display facilities and assistances, and Dr. Iain Manfield for the excellent technical support in SPR assay analysis, and the Wellcome Trust grant (062164/Z/00/Z) for funding the BIACORE3000 instrument, and Dr. Jack Goode, Mr. Duncan Sharp and Mr. Juan Leva Bueno for the technical assistance in electrochemical analysis. Thanks also go to Dr. Mohd Zulkifli Mustafa for editorial assistance.